Materials Research. 2022; 25:e20220161
DOI: https://doi.org/10.1590/1980-5373-MR-2022-0161

Evaluation of Abrasive WearRate and Machining Behaviors of Synthesized Nitinol Composite

S. Sridhar[a]*, S. Marichamy[b], Ram Subbiah[c]

[a]PSNA College of Engineering and Technology, Department of Mechanical Engineering, Dindigul, Tamilnadu, India.
[b]Sri Indu College of Engineering and Technology, Department of Mechanical Engineering, Hyderabad, Telangana, India.
[c]Gokaraju Rangaraju Institute of Engineering & Technology, Department of Mechanical Engineering, Hyderabad, Telangana, India.

Received: March 25, 2022; Revised: June 5, 2022; Accepted: July 19, 2022

The present investigation deals with wear and machining behaviors of manufacture nitinol composite through Vacuum Induction Melting (VIM). The major composition of nickel and titanium was reinforced with tungsten carbide (WC). Scanning Electron Microscopy (SEM) was employed to investigate the morphology of the synthesized nitinol composite. For investigating the topography of the surface of the nitinol composite was analyzed by scanning force microscopy or atomic force microscopy. Spark erosion machining has been applied to explore the machining behavior of the nitinol composite. Abrasive Wear Rate (AWR) is evaluated by using abrasion tester. Machining and wear parameters are optimized by applying taguchi approach. The contribution and the effect of input constraints on the responses are investigated by analysis of variance.Optimal abrasive wear rate was attained at 900 rpm of disc speed, 12 gm/min of abrasive flow rate and 400m of sliding distance. Disc speed was a dominant factor and it has developed 43.86% effect on abrasive wear rate. Optimal rate of metal removal was achieved at 45A of current, 200µs of pulse on time and 35V of Volts. The current was the leadingfactor and it has produced 86.38% effect on the rate of metal removal.

Keywords: *Nitinol composite, abrasive wear rate, machining characteristics, Surface topography, Taguchi approach.*

1. Introduction

The performance of the material has been enhanced by using alloying elements such as nickel and titanium. The malleable, hardand ductile properties have been enhanced through accumulation of nickel. The lightweight, high-strength and corrosion have been enhanced through accumulation of titanium. Moreover, material and substance properties have been developed by using tungsten carbide. It is used in heat engine temperature controls, microphone, springs, sheet metal works and medical industries[1]. It is pertinent to state that the durability and the reliability shown by nitinol alloy in extensive range of temperature applications andintransmission system of automobile have been excellent. Nitinol alloy contains superiormicro structureand exhibits better mechanical and electrical properties[2,3]. For actuator technologies and smart engineering structures, the role played by nitinol alloy got increased owing to outstanding thermo-mechanical performances and shape memory characteristics[4-6]. The crystal structures, substance properties and shape-memory behavior had been investigated in nitinol alloy under different conditions[7,8]. The recent developments, fabrication methods and applications of nitinol composite for aerospace had been analyzed[9,10]. Thermal behavior and its phase transformation of nitinol alloy had been investigated under different temperature conditions[11,12]. The material properties and the fabrication method of nitinol composite such as vacuum-melting technique have been analyzed[13]. The deformation and the tension behavior of nitinol alloy under compression and different phase transformation were investigated[14].The effect of microstructure and its behaviors of nitinol alloy had been related to martensitic transformation under different cyclic loading conditions[15,16]. The tribological characteristics and their effect on surface texture were investigated on tungsten carbide basedaluminum composite under different loads and sliding velocity[17]. The spark erosion behaviors of duplex brass and their responses such as rate of metal removal, surface texture were analyzed under different input constrains[18]. The different synthesis techniques of aluminium composite and their quality characteristics were optimized by Taguchi method. The wear behaviors of titanium boride based aluminium composite and their quality characteristics were optimized by Taguchi technique[19,20].

The present topic has been used to assess the abrasive wear rate and spark erosion machining behaviors of synthesized nitinol composite by employing vacuum induction meltingmethod. For accomplishing it, the material characterization, composition and surface morphologyhad been studied. Taguchi method has been employed to optimize the abrasive wear and spark erosion machining process parameters.

*e-mail: sri_2855@yahoo.co.in

2. Fabrication of Composite

In vacuum induction melting process, the graphite crucible has been considered for fabricating thecomposite. It has been used to fabricate composite with homogeneous chemical compositionand low impurity content[21]. High purity of metal can be achieved by employing vacuum induction melting method. Induction melting functions are based on induced electrical eddy currents. In the experimental investigation, 54.5 weight percentage of nickel, 44 weight percentage of titanium and 1.5 weight percentage of tungsten carbide have been used to fabricate nitinol composite.The different factors are used to affect the fabrication of nitinol composite such as material properties, composition of alloying elements, fabrication methods and reinforced particle properties. Tungsten carbide has very high strength. It has excellent resistance to deformation, deflection, impact, wear and oxidation. The tungsten carbide was pre heated and added to the alloy. The alumina or magnesia is not suitable due to contamination with molten nitinol composite. The carbon content has been controlled in a graphite crucible furnace at 1500°C. The transformation temperature is controlled in a graphite crucible furnace at 1495 - 1500°C. The furnace was sufficiently provided with air tight water cooled steel jackets and it is capable of withstanding more vacuum while processing materials.The heat energy has been applied to melt the nitinol composite through electromagnetic induction. The vacuum or inert gas environment was considered for pouring the molten metal to the cast iron mold. The substance properties and the refined microstructure were obtained in electromagnetic induction by using directional solidification process[22]. Vacuum induction melting has been used in different applications due to maintenance of thermodynamic stability and thermal shock resistance[23].

3. Material Characterization

The material structure and morphology was studied with the support of SEM images and the same is shown in Figure 1. It has been derived by employing vacuum induction melting process for synthesizing nitinol composite form.Greater reinforcement and its strength were developed between nickel and titanium. The tungsten carbide particles were located on the surface of the nitinol composite. The distribution of tungsten carbide particles along the surface has been homogeneous. Greater bonding interfacial strength has been achieved between alloys and tungsten carbide. The continuous formation of surface has been developed through deposited layers. The homogeneous surface mainly depends on the number of layers formed among the alloying elements[24]. The composition of alloying elements with tungsten carbide has been validated through EDAX and the same is shown in Figure 2.

4. Results and Discussion

4.1. Surface topography

Surface topography has been investigated by using Scanning Force Microscopy (SFM)and the same is shown in Figure 3.It is used to predict the topography of the surface and the functional properties of the material. Both image peak and valley surface profile have been identified with the maximum of 97μm. From the AFM image, the depth of penetration of the particles was observed to be maximized. The surface morphology and the penetration of the particles have been investigated on stainless steel[25]. The extruded surface profile of the composites was clearly represented in the AFM image and it confirms with the particles extruded with more than 90μm. The particle size and roughness was calibrated by using line profile and it is clearly evident that the mean area size of the particle was more than 500 μm area.

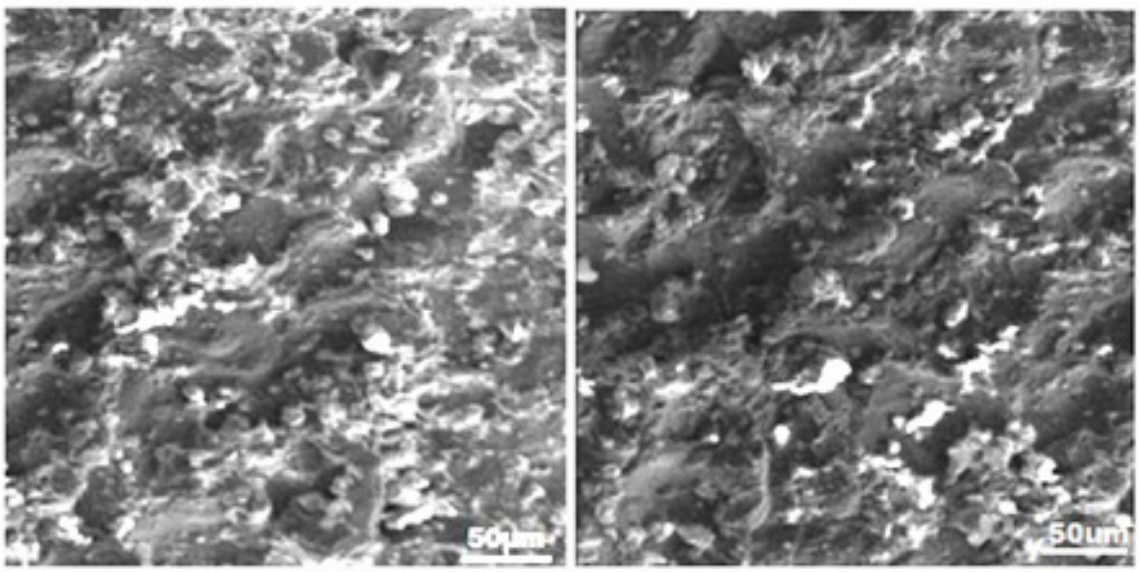

Figure 1. SEM images of synthesized Nitinol composite.

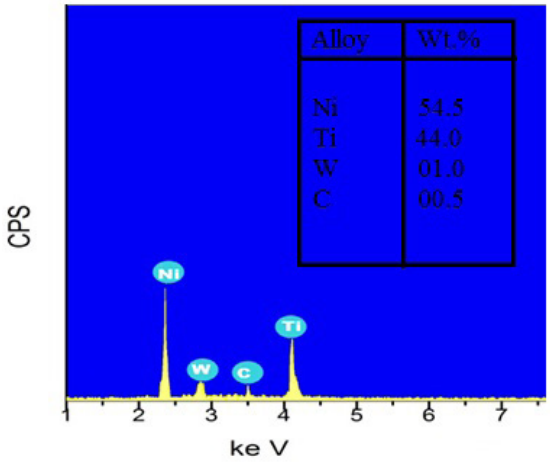

Figure 2. EDAX image of synthesized Nitinol composite.

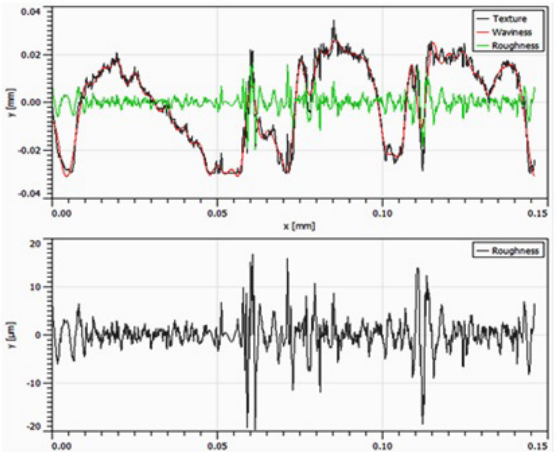

Figure 4. Surface plot of Nitinol composite.

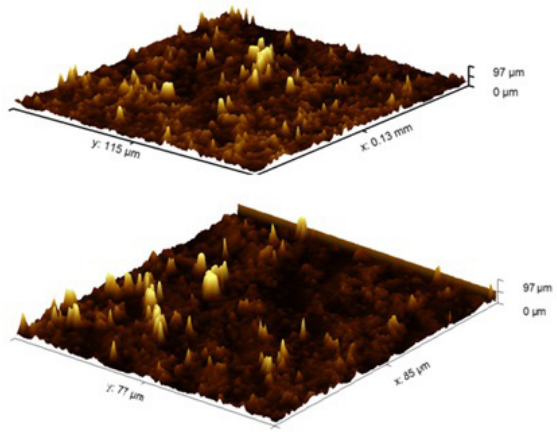

Figure 3. Scanning force microscopy of Nitinol composite.

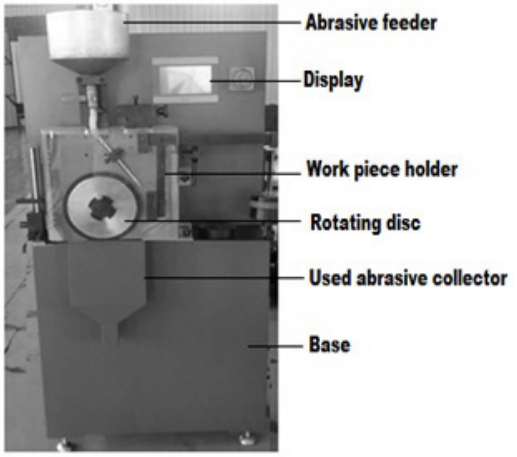

Figure 5. Dry sand rubber abrasion tester.

Surface plot is shown in Figure 4. Both surface characteristics and its roughness were analyzed in steel by using surface plot[26].Here, the image consists of more peak and valley profiles. It was investigated by employing several parameters and its surface was identified as smooth profile. In the image, a maximum height in roughness was observed at 36.53µmvalue and maximum height of the profile was observed at 36.25 µm value.

4.2. Abrasive wear test

Dry sand rubber abrasion tester has been employed to study the abrasive wear behaviors and the same has been shown in Figure 5. A Korean make with 15 KW abrasion testing machine was used. The rotating disc, abrasive feeder, work piece holder and used abrasive collector are the main components of abrasion apparatus. The rotating disc was fabricated by using dry sand rubber coupled through electric motor. The work piece was locatedbetweenthe rotating disc and the specimen holder. Abrasive particle of tantalum carbide was applied between the rotating disc and the nitinol composite.Tantalum carbide shows superior structural and mechanical properties. It provides higherwear and temperature resistance[27,28].

Abrasive wear rate was evaluated through different input constraints such as disc speed (300-900rpm), abrasive flow rate (4-12 gm/min) and sliding distance (400-800m). The experimental outcomes for abrasive wear rateare shown in Table 1. The experimentation was performed as per L9 orthogonal array. From the table, it is understood that the abrasive wear rate increased with an increase in disc speed and abrasive flow rate. The different process factors were taken into consideration for evaluating the abrasive wear resistance and disc rotational speed is the essential factor in affecting the abrasive wear resistance[29]. The large amount of particles were eroded from the surface of the workpiece was depending on high flow rate of abrasives[30].

4.3.Taguchi approach on abrasive wear rate

For evaluating the optimal factor of abrasive wear rate,it has been decided to employTaguchiexperimental

design. By applying Taguchiexperimental design, it has become possible to improve the quality characteristics of the responses depending on the input constraints. Abrasive wear rate of the material needs to be minimized for every material so as to attain better performance. Hence, lower the better criterion was considered to evaluatethe abrasive wear rate. The experimental results of disc speed, abrasive flow rate and sliding distance weretransformed into SN ratio and it was used toevaluate the abrasive wear rate[31]. The response of the means and the SN ratio has been shown in Table 2.

SN ratio effect on abrasive wear rate is shown in Figure 6. The optimal abrasive wear rate has been identified at disc speed of 900 rpm, abrasive flow rate of 12 gm/min and sliding distance of 400m.

Analysis of variance isshown (Table 3) along with the effect and the role of each input constraint on abrasive wear rate. The abrasive wear rate depends on disc speed, flow rate of abrasive and sliding distance. The largest contribution factoris found as disc speed. It has produced 43.86% effect on abrasive wear rate. The least contribution factor is found as sliding distance. It has produced 21.05% effect on abrasive wear rate. The wear rate gets increased with an increase in disc speed due to abrasive erosion. High amount of frictional heat got developed between rotating disc and the work piece due to sliding interface[32].

5. Spark Erosion Behaviors

Sparkonix model EDM has been employed to evaluate the machining behaviors of nitinol composite and it is shown in Figure 7. In EDM process, spark erosion principle has been used to remove the material from the work piece. The copper tungsten electrode has been employed as the tool material. EDM oil 30 has been used as the dielectric fluid. Holes with 6mm diameters were developed on the surface

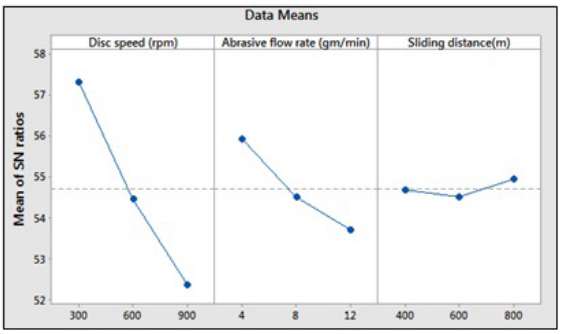

Figure 6. SN ratio effect on abrasive wear rate.

Figure 7. Spark erosion machining of nitinol composite.

Table 1. Experimental outcomes for abrasive wear rate.

Sl.No	Disc speed (rpm)	Abrasive flow rate (gm/min)	Sliding distance(m)	Abrasive wear rate (m^3/m)
1	300	4	400	0.00123
2	300	8	600	0.00145
3	300	12	800	0.00157
4	600	4	600	0.00175
5	600	8	800	0.00198
6	600	12	400	0.00218
7	900	4	800	0.00209
8	900	8	400	0.00253
9	900	12	600	0.00284

Table 2. SN ratio and Means for abrasive wear rate.

Level	SN ratio			Means		
	Disc speed	Flow rate	Sliding distance	Disc speed	Flow rate	Sliding distance
1	57.32	55.93	54.67	0.001367	0.001633	0.001933
2	54.46	54.51	54.52	0.001900	0.001933	0.001967
3	52.36	53.70	54.96	0.002433	0.002133	0.001800
Delta	4.96	2.23	0.44	0.001067	0.000500	0.000167
Rank	1	2	3	1	2	3

Table 3. Variance analysis for abrasive wear rate.

Source	DF	Adj. SS	Adj. MS	F-Value	P-Value	Percentage %
Disc speed	2	0.0000025	0.0000012	93.26	0.011	43.86
Abrasive flow rate	2	0.0000014	0.0000007	21.11	0.045	24.56
Sliding distance	2	0.0000012	0.0000006	1.57	0.389	21.05
Error	2	0.0000006	0.0000003	---	----	10.53
Total	8	0.0000057	----	---	----	100

of the nitinol composite by varying the input constraints of the spark erosion machining process. The size of the nitinol composite plate is 60x40x5mm.

The rate of material removal is evaluated and it is shown in Table 4. Various levels of input constraints were considered for current (15-45A), pulse on time (150-200 µs) and voltage (30-45V). L9 orthogonal array was applied to form the experimental design and accomplish the experiments. The rate of material removal got increased with an increase in current and pulse on time due to increase in spark intensity and stable metal erosion.

5.1. Taguchi approach on rate of material removal

The quality characteristics of the responses depended on taguchi experimental design. Rate of material removal got increased due to higher intensity of powerful spark produced between electrode and work piece. The material removal needs to be maximized to drill on the surface of the nitinol composite. Therefore,a large criterion was considered to besuitable for spark erosion machining process. The SN ratios and the means were performed as per the larger criterion considered to be better and the same was listed in Table 5.

The Figure 8 exhibits the main causes of SN ratio on rate of metal removal in nitinol composite. The optimal rate of metal removal is found at 45Acurrent, 200µs pulse on time and 35V voltage.

The rate of material removal depends on the input constraints of spark erosion process. RMR is directlyproportionate to the effect of current. It has developed 86.38% effect on rate of metal removal followed by other factors and the same is shown in Table 6. Pulse durationproduced moderate effect on rate metal removal. The voltage (1.89%) was the least factor on rate of metal removal. The rate of material removal got increased with an increase in current due to huge generation of arc and heat intensity[33]. The spark

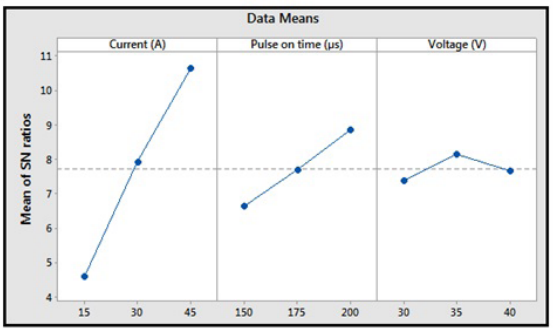

Figure 8. SN ratio effect on RMR.

Table 4. Experimental outcomes for RMR.

Exp.No.	Current (A)	Pulse on time (µs)	Voltage (V)	RMR (mm^3/min)
1	15	150	30	1.37
2	15	175	35	1.78
3	15	200	40	2.01
4	30	150	35	2.41
5	30	175	40	2.35
6	30	200	30	2.72
7	45	150	40	2.98
8	45	175	30	3.41
9	45	200	35	3.87

Table 5. SN ratios and Means for drilling of holes.

Level	SN ratio			Means		
	Current	Pulse on time	Voltage	Current	Pulse on time	Voltage
1	4.602	6.620	7.360	1.720	2.253	2.500
2	7.918	7.695	8.134	2.493	2.513	2.687
3	10.631	8.837	7.657	3.420	2.867	2.447
Delta	6.029	2.217	0.774	1.700	0.613	0.240
Rank	1	2	3	1	2	3

Table 6. Variance analysis for input constraints for machining process.

Source	DF	SS	MS	F	P	%
Current	2	4.34676	2.17338	203.54	0.005	86.38
Pulse on time	2	0.56862	0.28431	26.63	0.036	11.30
Voltage	2	0.09529	0.04764	4.46	0.183	01.89
Error	2	0.02136	0.01068	--	--	00.43
Total	8	5.03202	--	--	--	100

intensity, dielectric breakdown and arcing discharge were controlled by current[34].

6. Conclusion

While evaluating the abrasive wear rate and the spark erosion machining behaviors of synthesized nitinol composite through vacuum induction melting and optimization, the following conclusions were made:

- The tungsten carbide based nitinol composite got synthesized through vacuum induction melting process.
- Nitinol composite characterization and its alloying composition got confirmed through SEM and EDAX.
- The surface topography got investigated by employing scanning Force Microscopy and surface roughness got analyzed through surface plot.
- Abrasive wear test was conducted on nitinol composite. The optimal abrasive wear rate was found at 900 rpmof disc speed, 12 gm/minof abrasive flow rate and 400m of sliding distance.
- Disc speed was a powerful factor and it hasproduced 43.86% effect on abrasive wear rate.
- Spark erosion behaviors were evaluated in nitinol composite.The optimal rate of metal removal was found at 45A of current, 200µs ofpulse on time and 35V of Volts.
- The current was the predominant factor and it has produced 86.38% effect on the rate of metal removal.
- From the AFM image, peak and valley surface profile have been observed with the maximum of 97µm.The particles extruded with more than 90µm. From the surface plot, the maximum height of the roughness was observed at 36.53µm.

7. References

1. Lee ES, Shin TH. An evaluation of the machinability of nitinol shape memory alloy by electrochemical polishing. J Mech Sci Technol. 2004;25(4):963-70.
2. Barik L, Samal S, Behera A, Rajak DK, Pruncu CI. On the replacement of steel by NITINOL as coupling agent in automobile shaft. J Micro Smart Syst. 2021;10(2):87-102.
3. Shimoga G, Kim TH, Kim SY. An intermetallic NiTi-based shape memory coil spring for actuator technologies. Metals. 2021;11(8):1212-22.
4. Wadood A. Brief overview on nitinol as biomaterial. Adv Mater Sci Eng. 2016;1:110-7.
5. Abubakar RA, Wang F, Wang L. A review on Nitinol shape memory alloy heat engines. Smart Mater Struct. 2020;30:113-20.
6. Wang Z, Everaerts J, Salvati E, Korsunsky AM. Evolution of thermal and mechanical properties of Nitinol wire as a function of ageing treatment conditions. J Alloys Compd. 2020;819:153-60.
7. Huang X, Ackland GJ, Rabe KM. Crystal structures and shape-memory behaviour of NiTi. Nat Mater. 2003;2(5):307-11.
8. Jani JM, Leary M, Subic A. Designing shape memory alloy linear actuators: a review. J Intell Mater Syst Struct. 2016;28(13):1699-718.
9. Costanza G, Tata ME. Shape memory alloys for aerospace, recent developments, and new applications: a short review. Mater. 2020;13(8):1856-61.
10. Soother DK, Daudpoto J, Chowdhry BS. Challenges for practical applications of shape memory alloy actuators. Mater Res Express. 2020;7(7):173-80.
11. Sgambitterra E, Maletta C, Furgiuele F. Investigation on crack tip transformation in NiTi alloys: effect of the temperature. Shap MemSuperelasticity. 2015;1(2):275-83.
12. Sgambitterra E, Maletta C, Furgiuele F. Temperature dependent local phase transformation in shape memory alloys by nanoindentation. Scr Mater. 2015;101:64-7.
13. Pelton AR, Russell SM, DiCello J. The physical metallurgy of nitinol for medical applications. J Mater. 2013;55:33-7.
14. Bucsek AN, Paranjape HM, Stebner AP. Myths and truths of nitinol mechanics: elasticity and tension-compression asymmetry. Shap. Mem. Superelasticity. 2016;2(3):264-71.
15. Kimiecik M, Jones JW, Daly S. The effect of microstructure on stress-induced martensitic transformation under cyclic loading in the SMA Nickel-Titanium. J Mech Phys Solids. 2016;89:16-30.
16. Padula S 2nd, Qiu S, Gaydosh D, Noebe R, Bigelow G, Garg A, et al. Effect of upper-cycle temperature on the load-biased, strain-temperature response of NiTi. Metall Mater Trans, A Phys Metall Mater Sci. 2012;43(12):4610-21.
17. Arivukkarasan S, Dhanalakshmi V, Stalin B, Ravichandran M. Mechanical and tribological behaviour of tungsten carbide reinforced aluminum LM4 matrix composites. Particul Sci Technol. 2018;36(8):967-73.
18. Marichamy S, Stalin B, Ravichandran M, Sudha GT. Optimization of machining parameters of EDM for α-β brass using response surface methodology. Mater Today Proc. 2020;24(1):1400-9.
19. Stalin B, Sudha GT, Ravichandran M. Optimization of powder metallurgy parameters for AA7072-MoO_3 composites through taguchi method. Mater Today Proc. 2020;22(1):2622-30.
20. Chattoraj, P., Prabhakar, P., Koti, V., Natarajan, N. S., Lakshminarayana, M., Arul, K., Venkatachalapathy, M., Ahamed, M., Karnan, M., & Kumar, S. P. (2022). Optimization on tribological behaviour of AA7178/Nano Titanium Diboride Hybrid Composites Employing Taguchi Techniques. *Journal of Nanomaterials*, 1, 120-128.
21. Min PG, Vadeev VE. Vacuum induction furnace melting technology for high-temperature composite material based on Nb–Si system. Metallurgist. 2019;63(7-8):878-84.
22. Yan Y, Ding H, Kang Y, Song J. Microstructure evolution and mechanical properties of Nb–Si based alloy processed by electromagnetic cold crucible directional solidification. Mater Des. 2014;55:450-5.
23. Fashu, S., Lototskyy, M., Davids, M. W., Pickering, L., Linkov, V., Tai, S., Renheng, T., Fangming, X., Fursikov, P. V., & Tarasov, B. P. (2020). A review on crucibles for induction melting of titanium alloys. *Materials & Design*, 186, 108295.
24. Ba, K., Chahine, A., Ebn Touhami, M., Alauzun, J. G., & Manseri, A. (2020). Preparation and characterization of phosphate-nickel-titanium composite coatings obtained by sol–gel process for corrosion protection. *SN Appl Sci.*, 2(3), 350-360.
25. Bowen WR, Lovitt RW, Wright CJ. Atomic force microscope studies of stainless steel: surface morphology and colloidal particle adhesion. J Mater Sci. 2001;36(3):623-9.
26. Sachin B, Rao CM, Naik GM, Puneet NP. Influence of slide burnishing process on the surface characteristics of precipitation hardenable steel. SN Appl Sci. 2021;3(2):223-30.
27. Simonenko EP, Simonenko NP, Ezhov YS, Sevastyanov VG, Kuznetsov NT. Study of the synthesis of nanocrystalline mixed tantalum–zirconium carbide. Phys At Nucl. 2015;78(12):1357-65.
28. Kostenko, M. G., Gusev, A. I., & Lukoyanov, A. V. (2022). Structural and mechanical properties of predicted vacancy ordered tantalum carbide phases. *Acta Materialia*, 223, 117449.
29. Strzałkowski P, Kaźmierczak U, Wolny M. Assessment of the method for abrasion resistance determination of sandstones

on Böhme abrasion test apparatus. Bull Eng Geol Environ. 2020;2020(79):4947-56.
30. Medyński D, Janus A. Effect of heat treatment parameters on abrasive wear and corrosion resistance of austenitic nodular cast iron Ni-Mn-Cu. Arch Civ Mech Eng. 2018;18(2):515-21.
31. Soy U, Ficici F, Demir A. Evaluation of the Taguchi method for wear behavior of Al/SiC/B4C composites. J Compos Mater. 2012;46(7):851-9.
32. Li G, Hao S, Gao W, Lu Z. The effect of applied load and rotation speed on wear characteristics of Al-Cu-Li alloy. J Mater Eng Perform. 2022;1(7):146-55.
33. Moudood MA, Sabur A, Mohammad YA, Jaafar IH. Effect of peak current on material removal rate for electrical discharge machining of non-conductive Al_2O_3 ceramic. Adv Mat Res. 2013;845:730-4.
34. Oßwald K, Brandl L, Lochmahr I. Experimental investigation into material removal mechanisms in High Speed Wire EDM. Int J Adv Manuf Technol. 2020;2020(111):2163-70.